

# An Improved Rotor Position Estimation Method for SPMSM with Misaligned Hall-Effect Sensor

Xiaofeng Xu, Xiaoyan Huang, *Member, IEEE*, Qichao Hu, Zhaokai Li, *Member, IEEE*

**Abstract**—This paper presents an improved rotor position estimation method for surface permanent magnet synchronous motor (SPMSM) using a low-resolution Hall-Effect sensor. Firstly, an observation function is proposed to detect the speed variation, and a novel correction method based on optimization process is proposed to identify and correct the deviation angle caused by sensor misalignment. Then, an improved position observer is introduced using a gain-scheduling controller to achieve better performance in both steady state and transient state. The proposed method enhances the anti-perturbation and start-up capability for SPMSM and compensates the misalignment effect of Hall-Effect sensors. Experimental results are demonstrated to verify the effectiveness of the proposed method.

**Index Terms**—SPMSM, hall-effect sensor, sensor misalignment correction, position estimator.

## I. INTRODUCTION

ACCURATE rotor position is the key to the excellent performance of motors using vector control. High-precision position sensors are often expensive, and the sensorless methods draw intensive attention in the industrial application [1]. However, it performs poorly at the low-speed high-torque work condition and lacks stability. In some applications with requirements for high reliability, such as electric bikes [2] and home appliances [3], hall sensors are widely used due to their low cost and small compact size with simple information about rotor position. It is a compromise solution between reliability and cost.

For motor control systems using hall-effect sensors, sensor misalignment is a common problem, leading to a series of negative effects such as torque ripple and current distortion. The effects of unbalanced hall sensors [4] and torque ripple for electric vehicles [5] caused by rotor position error are investigated comprehensively. In order to reduce the effect of sensor fault, the methods proposed in [6]- [8] use the period or harmonics of the hall signal to diagnose and compensate for sensor fault. Additionally, a modified assisted rotor is

An earlier version of this paper was presented at 2022 IEEE Transportation Electrification Conference and Expo, Asia-Pacific (ITEC Asia-Pacific 2022), Haining, China, Oct.28-31.

This work was supported in part by the National Key R&D Program of China(2019YFE0123500), in part by the National Natural Science Foundation of China(51890883), in part by the Zhejiang Provincial Ten-Thousand-Talent Plan under Grant (2019R52003)and in part by the Zhejiang Provincial Natural Science Foundation of China under Grant No. LQ22E070003.

Xiaofeng Xu, Xiaoyan Huang and Qichao Hu are with Zhejiang Provincial Key Laboratory of Electrical Machine Systems, College of Electrical Engineering, Zhejiang University, Hangzhou 310027, China (e-mail: xiaofengxu@zju.edu.cn; xiaoyanhuan@zju.edu.cn; eehqc@zju.edu.cn). Zhaokai Li is with Department of Electrical Engineering, KTH Royal Institute of Technology, Stockholm, 11428, Sweden (zhaokai@kth.se).

proposed in [9] to solve abnormal hall sensor problems caused by leakage flux, and the wavelet signal theory [10] and error on current harmonics [11] can also be used for fault diagnosis. For correction methods, an error compensation controller is proposed in [12] with an integral model to compensate error at each sector separately, and the fault-tolerant control proposed in [13] can compensate the redundant hall sensors within electrical 30°. However, the above methods [6]- [13] focus more on fault-tolerant control strategies and less on angular deviations, especially those caused by installation misalignment.

Three phase hall-effect sensors can only detect six different states and give the accurate position for every 60° electrical angle. The methods to improve the accuracy of the estimation angle can be summarized into two categories. The first one is named as predictive method, of which the average speed method [14] and the acceleration method [15] are representative. As these methods use the speed information calculated from the hall signal to estimate rotor position, they can achieve good steady-state performance. However, they are vulnerable to disturbances in transient process. The polynomial fitting and interpolation are used to estimate rotor position through information processed by hall signals [16] [17], but there is a time delay in the dynamic processes. To achieve a more economical servo system application, the method in [18] combines a double sampling observer and polynomial fitting to decouple the position and speed observer. For electric vehicle applications, a more practical moving average manner is proposed in [19], and an improved method is applied for low-cost electric vehicles with compensation for misplaced hall sensors [20]. However, the response time of these methods is affected when the motor operates unstably.

The second one is the observer method, where the observer is designed to extract information about rotor position and speed from hall signals. The observer method often requires the analysis of the harmonic components of the hall signal [21]- [23], and the useful information of speed and rotor angle is extracted from the harmonic components to improve the observer effect. In [24], a vector tracking observer with the average speed as feedforward is proposed to detect position error based on the vector cross product of a back-electromotive-force (BEMF) vector. The speed and disturbance under low-resolution encoders are estimated by a dual-sampling-rate observer [25], and a dual observer without time delay is proposed in [26] to correct the mounting deviation of sensors. However, the complexity of the observer will bring high hardware costs.

The filtering method is another way to process the sensor signals directly [27], but it usually focuses on the steady-

state performance. Some sensorless methods tend to perform well when aided by binary hall-effect sensors based on the high-frequency injection in safety-critical systems [28], but the machine must possess sufficient electromagnetic saliency. To reduce the noise effects, a periodic interrupt method [29] is proposed that is insensitive to noise but whose performance is diminished when speed increases.

In this paper, in order to estimate the rotor position within a  $60^\circ$  electrical angle with the simple information from the hall sensor, an observation function obtained by an inner product operation is proposed to estimate the speed. Considering the effect of sensor misalignment, a correction method for the misalignment of hall sensor installation is first presented to identify the deviation angle of sensors, where an optimization problem is summarized due to the effect of sensor misalignment on the value of the observation function. After that, for the problem of time delay resulting from the traditional average speed method in the dynamic process, an improved position estimator with the average speed as feedforward input is proposed, which adopts the speed information obtained from the value of the observation function after correction to compensate for the average speed in the transient process, and can improve the accuracy of estimated rotor position. The effectiveness of the correction method for sensor misalignment and the position estimator is experimentally verified.

## II. MISALIGNED HALL-EFFECT SENSORS

### A. Features of Hall-Effect Sensors

One typical mounting method of hall-effect sensors is shown in Fig. 1. The resolution of the corresponding position information is low. For three hall sensors, there are six different hall states in one electrical cycle, which means that only a resolution of  $\pm 30^\circ$  electrical angle can be achieved. In addition, an accurate rotor position can also be obtained when the hall state is switched, as shown in Fig. 2(b). However, the accuracy of this angle depends on the actual installation location.

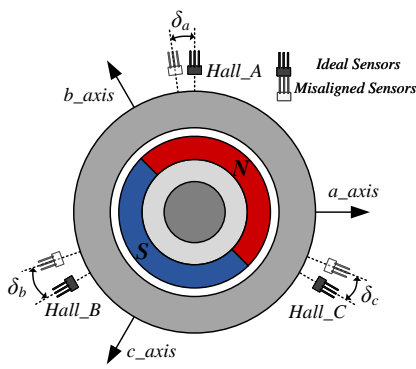


Fig. 1. Two-pole SPMMSM with misaligned hall-effect sensors.

### B. Adverse Effects of Hall Sensors Misalignment

If there is a deviation in the installation of the hall sensors or if faults occur in the signals processing circuit during operation, an offset between the actual hall signals and the

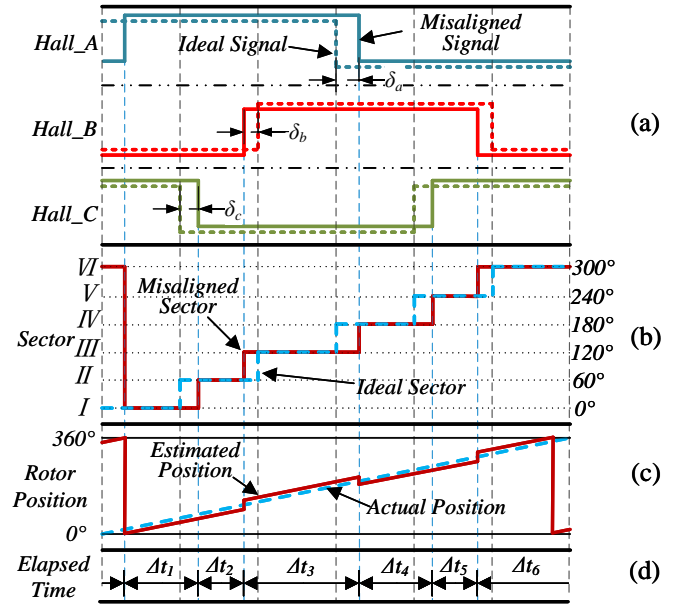


Fig. 2. Schematic of misaligned hall-effect sensors. (a) Output signal of ideal and misaligned sensors. (b) Six sectors classified by output signals. (c) Estimated and actual position. (d) Elapsed time of each sector.

ideal signals will be generated, resulting in errors in position estimation and unexpected elapsed time during each sector.

For example, assuming the deviations  $\delta_a$ ,  $\delta_b$ , and  $\delta_c$  of the sensors installation are equal to  $10^\circ$ ,  $-8^\circ$ , and  $4^\circ$  (The deviations are defined as positive when the ideal signal is ahead of the misaligned signal), respectively, as shown in Fig. 2(a) and 2(b), three misaligned sensors will cause the output signals to be delayed or advanced compared to the ideal signals when the sector changes. The problem of estimation error between the estimated position and the actual position will be magnified because of the sensor misalignment, as Fig. 2(c) displays that the angle error varies significantly in different sectors depending on the deviations  $\delta_a$ ,  $\delta_b$ , and  $\delta_c$ . In addition, the elapsed time will be inaccurate shown in Fig. 2(d), which is widely used to estimate speed.

## III. SENSOR MISALIGNMENT CORRECTION AND POSITION ESTIMATION

### A. Position Estimation with Average Speed Method

Six different states in one electrical cycle can be classified by different hall signals, and the duration of each sector can be used to calculate an average speed [14] [15]. The average speed and estimation position can be approximated as follows:

$$\omega_{avg(i)} = \frac{\pi/3}{\Delta t_{(i)}} \quad (1)$$

$$\theta_e = \theta_{s(i)} + n \cdot T_s \cdot \omega_{avg(i)} \quad (2)$$

where  $\omega_{avg(i)}$  is the calculated average speed for sector  $i$ ;  $\Delta t_{(i)}$  is the elapsed time of sector  $i$ ;  $\theta_e$  is the estimated rotor position;  $\theta_{s(i)}$  is the accurate position when the hall state switches from sector  $i$  to next sector;  $T_s$  is the sampling period of current loop; and  $n$  is the number of past sampling periods.

When the speed is constant in steady state, an accurate speed can be calculated using equation (1). With the accurate speed and the ideal position when the hall state changes, the precise rotor position can be estimated. However, once the motor speed changes due to load fluctuation or speed command, the average speed calculated under the dynamic process cannot reflect the actual speed without delay, which will cause an estimation error. Similarly, if there is a deviation during the sensor installation, a constant angular estimation error will be produced even if the calculated average speed is accurate.

### B. Proposed Sensor Misalignment Correction Method

An accurate rotor position is the basis for good performance of vector control, and the sensor deviation will bring a constant position estimation error that cannot be solved by improving the performance of the angle observer. Therefore, first a sensor misalignment correction method is proposed to solve the deviation problem, and on top of that, an improved rotor position estimation method is proposed.

The voltage equation of SPMMSM in  $\alpha\beta$ -axis can be expressed as:

$$\begin{bmatrix} u_\alpha \\ u_\beta \end{bmatrix} = \begin{bmatrix} R_s + pL_s & 0 \\ 0 & R_s + pL_s \end{bmatrix} \begin{bmatrix} i_\alpha \\ i_\beta \end{bmatrix} + \omega_e \psi_m \begin{bmatrix} -\sin\theta_e \\ \cos\theta_e \end{bmatrix} \quad (3)$$

The Euler Method is commonly used to discretize the model equation of the motor in general control strategies, but in order to achieve a more accurate identification of the sensor installation by estimating BEMF, an exact discretization of the voltage equation is presented as follows:

$$\begin{bmatrix} i_\alpha(k) \\ i_\beta(k) \end{bmatrix} = \mathbf{A} \begin{bmatrix} i_\alpha(k-1) \\ i_\beta(k-1) \end{bmatrix} + \mathbf{B} \begin{bmatrix} u_\alpha(k-1) \\ u_\beta(k-1) \end{bmatrix} + \mathbf{D}[k-1] \quad (4)$$

where

$$\mathbf{A} = \begin{bmatrix} e^{-\frac{T_s R_s}{L_s}} & 0 \\ 0 & e^{-\frac{T_s R_s}{L_s}} \end{bmatrix} \quad \mathbf{B} = \frac{1}{R_s} \begin{bmatrix} 1 - e^{-\frac{T_s R_s}{L_s}} & 0 \\ 0 & 1 - e^{-\frac{T_s R_s}{L_s}} \end{bmatrix}$$

$$\mathbf{D}[k-1] = \frac{\psi_f \omega_e[k-1]}{R_s^2 + L_s^2 \omega_e^2[k-1]} \cdot \left( \begin{array}{l} R_s \left[ \begin{bmatrix} \sin\theta_e[k] - e^{-\frac{T_s R_s}{L_s}} \sin\theta_e[k-1] \\ -\cos\theta_e[k] + e^{-\frac{T_s R_s}{L_s}} \cos\theta_e[k-1] \end{bmatrix} \right] - \\ L_s \omega_e[k-1] \left[ \begin{bmatrix} \cos\theta_e[k] - e^{-\frac{T_s R_s}{L_s}} \cos\theta_e[k-1] \\ -\sin\theta_e[k] + e^{-\frac{T_s R_s}{L_s}} \sin\theta_e[k-1] \end{bmatrix} \right] \end{array} \right)$$

It can be found that the item  $\mathbf{D}[k-1]$  in (4) contains the speed variable  $\omega_e[k-1]$ , rotor position variable  $\theta_e[k-1]$  and  $\theta_e[k]$ . Furthermore, the value of  $\mathbf{D}[k-1]$  can be calculated entirely from the current and voltage, where the current  $i_{\alpha(\beta)}$  is the sampling phase current after Clarke Transform and the voltage  $u_{\alpha(\beta)}$  is reconstructed using the method in [30] while the influence of inverter nonlinearity is considered. As a result, the value of  $\mathbf{D}[k-1]$  can be calculated using the following equation:

$$\mathbf{D}[k-1] = \begin{bmatrix} i_\alpha(k) \\ i_\beta(k) \end{bmatrix} - \mathbf{A} \begin{bmatrix} i_\alpha(k-1) \\ i_\beta(k-1) \end{bmatrix} - \mathbf{B} \begin{bmatrix} u_\alpha(k-1) \\ u_\beta(k-1) \end{bmatrix} \quad (5)$$

In a digital control system, one cycle time is relatively short, so the speed can therefore be considered constant, and the position could be written as:

$$\theta_e[k] = \theta_e[k-1] + \omega_e[k-1] \cdot T_s \quad (6)$$

The  $\mathbf{D}[k-1]$  obtained by equation (5) is a vector in two-dimensional space, and an angle vector  $\Theta[k-1]$  is used to reduce the variables.  $\Theta[k-1]$  is constructed using the estimated position in the control algorithm:

$$\Theta[k-1] = \begin{bmatrix} \sin\theta_e[k-1] \\ -\cos\theta_e[k-1] \end{bmatrix} \quad (7)$$

As a result, an observation function is proposed to extract the speed and position using the inner product of vectors, and it can be discovered that the value of the observation function can be obtained, whose ideal expression is:

$$f(\omega_e) = \Theta^T[k-1] \times \mathbf{D}[k-1] \quad (8)$$

$$= \frac{\psi_f \omega_e[k-1]}{R_s^2 + L_s^2 \omega_e^2[k-1]} \cdot (R_s (\cos(\omega_e[k-1] T_s) - e^{-\frac{T_s R_s}{L_s}}) + \omega_e[k-1] L_s \sin(\omega_e[k-1] T_s))$$

However, the accuracy of the angle vector  $\Theta[k-1]$  determines the correctness of the ideal observation function  $f(\omega_e)$ . When considering the sensor deviation, the installation error is expressed as  $\Delta\theta$ , and the exact position is  $\theta_e$ . A new angle vector  $\Theta_{error}[k-1]$  considering the misalignment is defined as follows:

$$\theta_{e\_error}[k-1] = \theta_e[k-1] + \Delta\theta \quad (9)$$

$$\Theta_{error}[k-1] = \begin{bmatrix} \sin(\theta_{e\_error}[k-1]) \\ -\cos(\theta_{e\_error}[k-1]) \end{bmatrix} \quad (10)$$

Therefore, when installation position errors are taken into account, equation (8) should be corrected to an expression named actual observation function with errors, as follows:

$$f_{error}(\omega_e, \Delta\theta) = \Theta_{error}^T[k-1] \times \mathbf{D}[k-1] \quad (11)$$

$$= \cos\Delta\theta \cdot f(\omega_e) + \sin\Delta\theta \cdot g(\omega_e)$$

$$\text{where } g(\omega_e) = \frac{\psi_f \omega_e[k-1]}{R_s^2 + L_s^2 \omega_e^2[k-1]} \cdot (R_s \sin(\omega_e[k-1] T_s) - L_s \omega_e[k-1] (\cos(\omega_e[k-1] T_s) - e^{-\frac{T_s R_s}{L_s}}))$$

The function  $g(\omega_e)$  is named as perturbation function. In the steady-state process, an improved average speed noted as  $\omega_{avg\_corr}$  is proposed in [20], which has a delay problem but is not affected by the installation deviation, so it can be used for misalignment correction. When sensor misalignment causes inaccurate elapsed time  $\Delta t_{(i)}$ , using  $\omega_{avg\_corr}$  for position estimation in (2) can exclude the influence of incorrectly calculated  $\omega_{avg(i)}$  by (1). The installation error  $\Delta\theta$  can be identified by comparing the actual observation function value  $f_{error}(\omega_e, \Delta\theta)$  and the ideal observation function value  $f(\omega_{avg\_corr})$  calculated with  $\omega_{avg\_corr}$ . And the correction steps are introduced in detail as follows:

#### 1) Step 1:

As shown in Fig. 1, three hall sensors' respective deviations lead to different widths of the hall sector, as shown concretely

in Table I. Firstly, in order to achieve a good identification effect, the angle of deviation in different sectors needs to be corrected to an identical angle.

TABLE I  
WIDTH OF SECTOR CONSIDERING SENSOR MISALIGNMENT

Hall Sector	Sector Width(°)	Elapsed Time(s)
I	$60 - \delta_a + \delta_c$	$\Delta t_1$
II	$60 + \delta_b - \delta_c$	$\Delta t_2$
III	$60 + \delta_a - \delta_b$	$\Delta t_3$
IV	$60 - \delta_a + \delta_c$	$\Delta t_4$
V	$60 + \delta_b - \delta_c$	$\Delta t_5$
VI	$60 + \delta_a - \delta_b$	$\Delta t_6$

According to the relationship between the rotor speed and angle, the following equation can be listed:

$$\begin{cases} [(\Delta t_1 + \Delta t_4)/2 - \Delta_t] \cdot \omega_{avg\_corr} = \delta_c - \delta_a \\ [(\Delta t_2 + \Delta t_5)/2 - \Delta_t] \cdot \omega_{avg\_corr} = \delta_b - \delta_c \\ [(\Delta t_3 + \Delta t_6)/2 - \Delta_t] \cdot \omega_{avg\_corr} = \delta_a - \delta_b \end{cases} \quad (12)$$

where  $\Delta_t = \frac{1}{6} \sum_{i=1}^6 \Delta t_i$ .

Since the system of equation (12) is linearly dependent, it can only be obtained:

$$\begin{cases} \delta_b = \delta_a - [(\Delta t_3 + \Delta t_6)/2 - \Delta_t] \omega_{avg\_corr} \\ \delta_c = \delta_a + [(\Delta t_1 + \Delta t_4)/2 - \Delta_t] \omega_{avg\_corr} \end{cases} \quad (13)$$

The correction of  $\delta_b$  and  $\delta_c$  in (13) can normalize the errors in different sectors to the same error  $\delta_a$ . Therefore, the actual observation function value derived from (11) will not fluctuate in different hall states.

## 2) Step 2:

When the overall error is a fixed value  $\delta_a$ , the actual observation function value  $f_{error}(\omega_e, \Delta\theta)$  containing the error remains constant in different sectors, so the correction of  $\delta_a$  can be summarized as an optimization problem:

$$\begin{cases} \min F(\Delta\theta) = f(\omega_{avg\_corr}) - f_{error}(\omega_e, \Delta\theta) \\ \text{s.t. } -30^\circ \leq \Delta\theta \leq 30^\circ \end{cases} \quad (14)$$

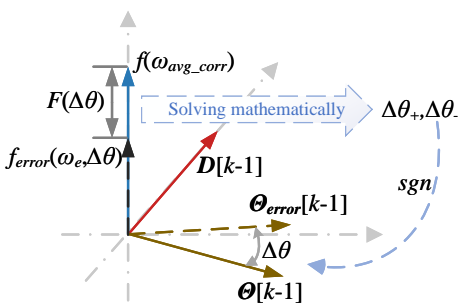


Fig. 3. Vector diagram of the optimization problem.

Fig. 3 depicts the vector diagram of the optimization problem. The observation function value is obtained by monitoring the operation state of the motor. However, the method of constantly changing parameter  $\Delta\theta$  in control algorithm to solve the optimization problem is inefficient and can also adversely affect the stability of the PMSM. To address this issue, the parameter  $\Delta\theta$  is solved mathematically based on the difference between the observation function value and its ideal value using an optimization-seeking method.

When the above optimization problem is solved purely mathematically, the target deviation angle  $\Delta\theta$  will have two solutions at  $[0^\circ, 30^\circ]$  and  $[-30^\circ, 0^\circ]$  noted as  $\Delta\theta_+$  and  $\Delta\theta_-$ , respectively. To determine the direction, it is only necessary to substitute a small correction value into the motor control system and observe the value of  $f_{error}(\omega_e, \Delta\theta + \Delta\theta_+)$ . If the error of measurement equation  $F(\Delta\theta)$  grows larger, it means that the direction has been misjudged. Finally, the error direction determined by the above method is indicated by the variable  $sgn$  in (15). After several numbers of iteration, the correction error of  $\delta_a$  can be obtained as follows:

$$sgn = \frac{f_{error}(\omega_e, \Delta\theta + \Delta\theta_+) - f_{error}(\omega_e, \Delta\theta)}{f_{error}(\omega_e, \Delta\theta + \Delta\theta_+) - f_{error}(\omega_e, \Delta\theta_+)} \quad (15)$$

where  $\Delta\theta_+^* = \Delta\theta_+/3$ .

$$\delta_a = \begin{cases} \Delta\theta_+, & sgn < 0 \\ \Delta\theta_-, & sgn > 0 \end{cases} \quad (16)$$

## C. An Improved Rotor Position Estimation Method

Since the observation function defined in (8) is univariate, the function value calculated by (8) can be used to calculate an estimated speed  $\omega_e^*$  using the Look-Up Table (LUT) method. However, the estimated  $\omega_e^*$  is vulnerable to the effects of noise and disturbance in steady processes when the current or speed fluctuates under complex operating conditions, so it cannot be used to directly estimate the angle. Therefore, an improved speed estimation observer that takes the average speed as feedforward is proposed. And the average speed  $\omega_{avg}$  (17) is calculated using hall signals that have been corrected for sensor misalignment. The delay problem of  $\omega_{avg}$  can be shortened when compared to the proposed speed  $\omega_{avg\_corr}$  in [20].

$$\omega_{avg(i)} = \begin{cases} \frac{\pi/3}{\Delta t_{(i)}} \cdot (1 + \frac{\delta_c - \delta_a}{60}), & i = 1, 4 \\ \frac{\pi/3}{\Delta t_{(i)}} \cdot (1 + \frac{\delta_b - \delta_c}{60}), & i = 2, 5 \\ \frac{\pi/3}{\Delta t_{(i)}} \cdot (1 + \frac{\delta_a - \delta_b}{60}), & i = 3, 6 \end{cases} \quad (17)$$

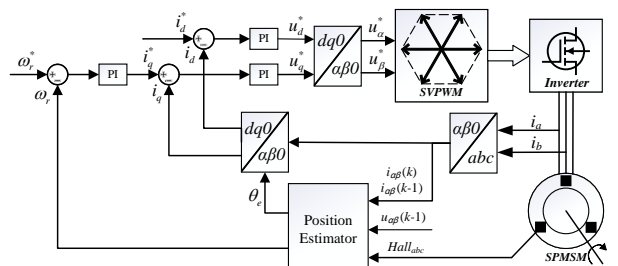


Fig. 4. Control scheme of SPMSM with the proposed rotor position estimation method.

The whole control scheme of SPMSM with the proposed rotor position estimation method is shown in Fig. 4, where the diagram of the position estimator is shown in Fig. 5. The speed estimation observer processes the speed  $\omega_e^*$  obtained from the LUT method, which has the same effect as a weighted filter. The average speed  $\omega_{avg}$  is accurate when estimating speed and rotor position in the steady-state process, but during

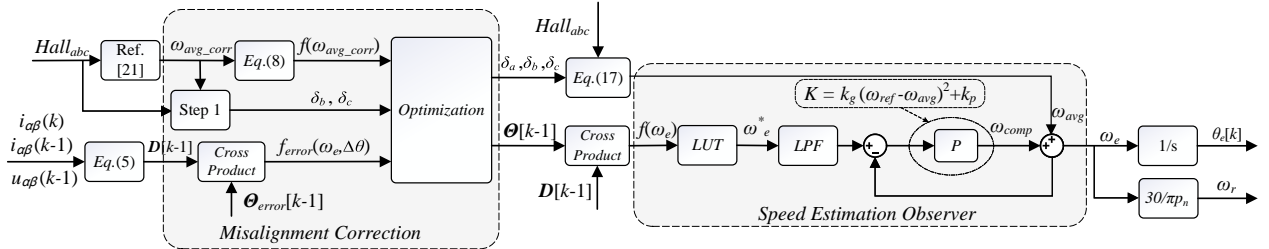


Fig. 5. Overall scheme of position estimator.

the dynamic process, large position estimation errors will be introduced as the average speed is unable to reflect the transient speed in the dynamic state.

A simple gain-scheduling proportional controller is used in the speed estimation observer. The purpose of the controller is mainly to improve dynamic performance. However, a fixed property of proportional gain cannot perform well in both dynamic and steady process. Therefore, a simple gain-scheduling coefficient  $K$  is proposed and given by the following equation:

$$K = k_g(\omega_{ref} - \omega_{avg})^2 + k_p \quad (18)$$

where  $\omega_{ref}$  is the given reference by speed loop;  $\omega_{avg}$  is the average speed calculated by (17);  $k_g$  and  $k_p$  are the fixed proportional gain.

The output of  $\omega_e$  can be express as:

$$\omega_e = \frac{K}{1+K}\omega_e^* + \frac{1}{1+K}\omega_{avg} \quad (19)$$

Theoretically, a larger  $K$  can achieve a shorter tracking delay, but the noise of  $\omega_e^*$  will also be magnified. Assuming that  $(\omega_{ref} - \omega_{avg}) > 1\% \cdot \omega_n$ , it is necessary to compensate for the average speed to achieve a balance of tracking delay and noise suppression. Therefore,  $k_g$  and  $k_p$  can be set as follows:

$$\begin{cases} k_g > \frac{10}{(0.01\omega_n)^2} \\ k_p < 0.5 \end{cases} \quad (20)$$

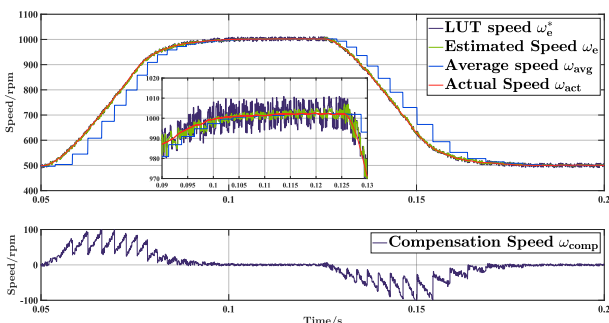


Fig. 6. The observer response during speed variation.

The role of the speed estimation observer is depicted in Fig. 6. It can be seen that there is a delay in the calculation of  $\omega_{avg}$  in the dynamic process, and the estimated speed  $\omega_e$  can be compensated by the output of proportional controller,

which is defined as  $\omega_{comp}$ . While in the steady-state process, the LUT speed  $\omega_e^*$  fluctuates and the average speed  $\omega_{avg}$  is accurate, the estimated speed  $\omega_e$  is primarily affected by  $\omega_{avg}$  with the proportional controller to suppress the noise in  $\omega_e^*$ .

The control algorithm of the proposed position estimation method is simple. Additionally, the method maintains the advantages of the average speed method in the steady-state process, and compensates for the shortcomings in the dynamic process through a simple feedforward structure to reduce the negative effects of system vibration caused by inaccurate angle estimation. Moreover, the proposed method is not sensitive to the changes of inductance, and both the effectiveness of sensor misalignment correction and proposed position estimator can maintain good performance when inductance variations occur.

#### IV. EXPERIMENTAL RESULTS

Several experiments are designed to verify the effectiveness of the proposed method. The experimental platform is shown in Fig. 7, and the control processor is the TMS320F28335 based on the TMDSHVMTRPFCKIT of TI. The SPMSM used in the experiments is equipped with both hall-effect sensor and an incremental encoder, and the specific parameters are shown in Table II. In the experimental scenarios, the measured speed and angle from the encoder are utilized as comparison values to validate the proposed method.

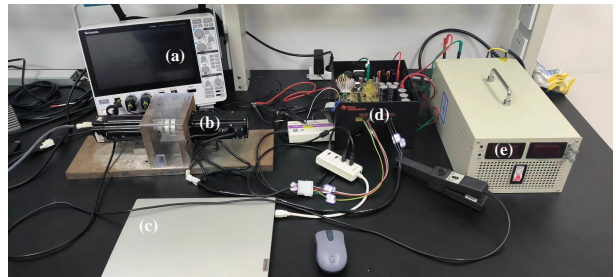


Fig. 7. Experimental platform. (a) Oscilloscope. (b) SPMSM. (c) Personal computer. (d) Driver controller board. (e) DC Power.

##### A. Performance of the Misalignment Correction Method

When there is an installation deviation of three hall sensors, the corresponding errors will exist between the estimated position and the actual position, as shown in Fig. 8. The wrong

TABLE II  
SPECIFICATION OF SPMSM

Description	Symbol	Value
Voltage	$V_{DC}$	220V
Nominal Speed	$\omega_n$	3000rpm
Torque	$T_e$	1.12N·m
Stator Resistance	$R_s$	2.45Ω
Stator Inductance	$L_s$	9.345mH
Flux Linkage	$\psi_f$	0.0593Wb
Number of Pole Pairs	$P_n$	4
Deviation of Hall_A	$\delta_a$	-7.2°
Deviation of Hall_B	$\delta_b$	-8.0°
Deviation of Hall_C	$\delta_c$	-6.6°

rotor position will worsen the effects of vector control and bring about problems such as current distortion and system vibration. Based on the proposed misalignment correction method, the Golden Division method commonly used in optimization is selected as the seeking algorithm.

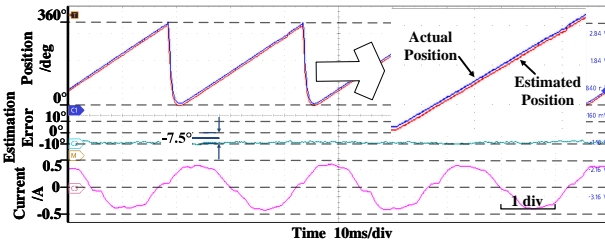


Fig. 8. Estimation error due to sensor misalignment of SPMSM.

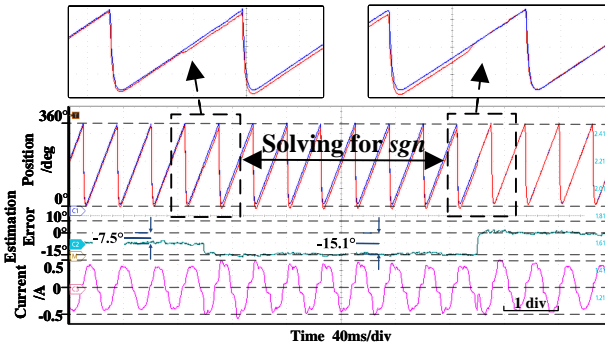


Fig. 9. The correction process.

The correction process is shown in Fig. 8, and the effect of Step 1 is not obvious because three halls' asymmetry of misalignment is small. To begin with, the left part of Fig. 9

depicts the identification process for the symbol  $sgn$ . Assuming the deviation angle to be  $\Delta\theta+$ , the positive or negative of  $sgn$  can be obtained according to the change of  $F(\theta)$  by (15), and the correction angle of  $\delta_a$  can be determined. And the right part of Fig. 9 shows the waveforms of the actual position and the estimated position after correction, and it can be seen that the estimated error is greatly reduced, and the THD of the phase current is also decreased. The comparison of the indicators before and after the correction is recorded in Table III.

TABLE III  
COMPARISON OF THE DEVIATION BEFORE AND AFTER CORRECTION

Symbol	Before	After
$\delta_a$	-7.2°	0.6°
$\delta_b$	-8.0°	1.0°
$\delta_c$	-6.6°	0.4°
THD of Current	17.64%	11.47%

To further illustrate the efficiency of the correction algorithm, a simulated hall signal processed by the signals of the incremental encoder is used to analyze the effect of the correction method when three halls have different and asymmetrical errors.

As shown in Fig. 10, the estimated rotor position has different errors in each sector when the three errors are -8°, 10°, and 4°, respectively. And Fig. 10(a) shows the process of correction in Step 1, which first normalizes the errors in different sectors and then corrects the uniform error, as shown in Fig. 10(b). The speed performed in Figs. 8, 9, and 10 for misalignment correction was 500 rpm.

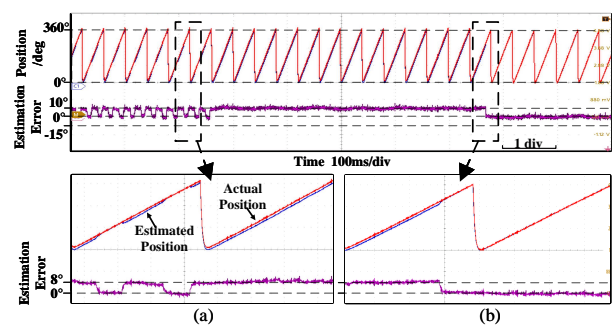


Fig. 10. Correction process when  $\delta_a = -8^\circ$ ,  $\delta_b = 10^\circ$ , and  $\delta_c = 4^\circ$ . (a) Step 1. (b) Step 2.

Fig. 11 shows the correction results for three hall sensors with various combinations of error, and the results demonstrate

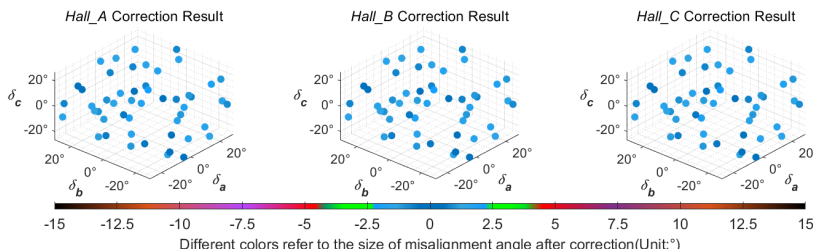


Fig. 11. Correction results of three hall sensors with different deviation angle.

that the correction method can perform well in different situations. By analyzing the specific algorithm, the correction effect of Step 1 to normalize the errors depends only on the  $\omega_{avg\_corr}$ , and the accuracy of  $\omega_{avg\_corr}$  cannot be affected by hall misalignment [20]. Therefore, different errors of the three halls will not couple with each other, which means that different combinations of errors do not influence the effect of the correction algorithm.

### B. Performance of Position Estimator

To analyze the performance of the proposed rotor position estimation method, a comparative experiment with the average speed method is presented, in which three dynamic processes including startup, speed reversal, and load variation are considered. As their common feature is the sudden change in rotor speed, the main contribution of the observer is to improve the accuracy of the speed estimation, further reduce the position estimation error, and improve the dynamic response performance.

Due to the low resolution of hall-effect sensors, the calculated results of the average speed method cannot reflect the actual speed without delay during dynamic process. As a result, the delay of speed observation leads to the temporary failure of the speed loop, and the current increases drastically. The above risks can be avoided by decreasing the PI parameters of the speed loop, but the dynamic responsiveness will also be reduced. The comparison of speed response and estimated position with two methods at startup is shown in Fig. 12. As Fig. 12(a) shows, the estimated position in the average speed method has a large error up to  $63.5^\circ$  and a longer convergence time of 56.0 ms. Comparatively, the effect of the proposed method has a more accurate estimated speed, a smaller current inrush, and a faster convergence time of 28.0 ms, as shown in Fig. 12(b).

For applications that require forward/reverse control of motor, during speed reversal the calculated average speed significantly lags behind the actual speed. When the speed is switching from positive to negative at a certain hall sector, the feedback speed is still the average speed calculated in the

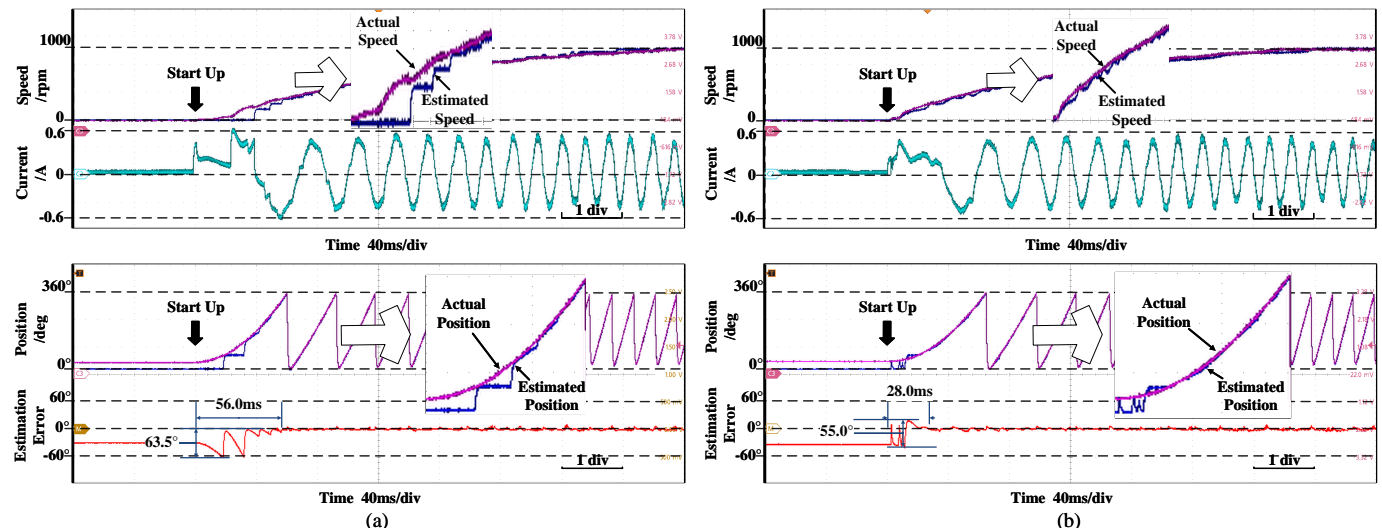


Fig. 12. Speed change from 0 to 1000 rpm. (a) With the average speed method. (b) With the proposed position estimator.

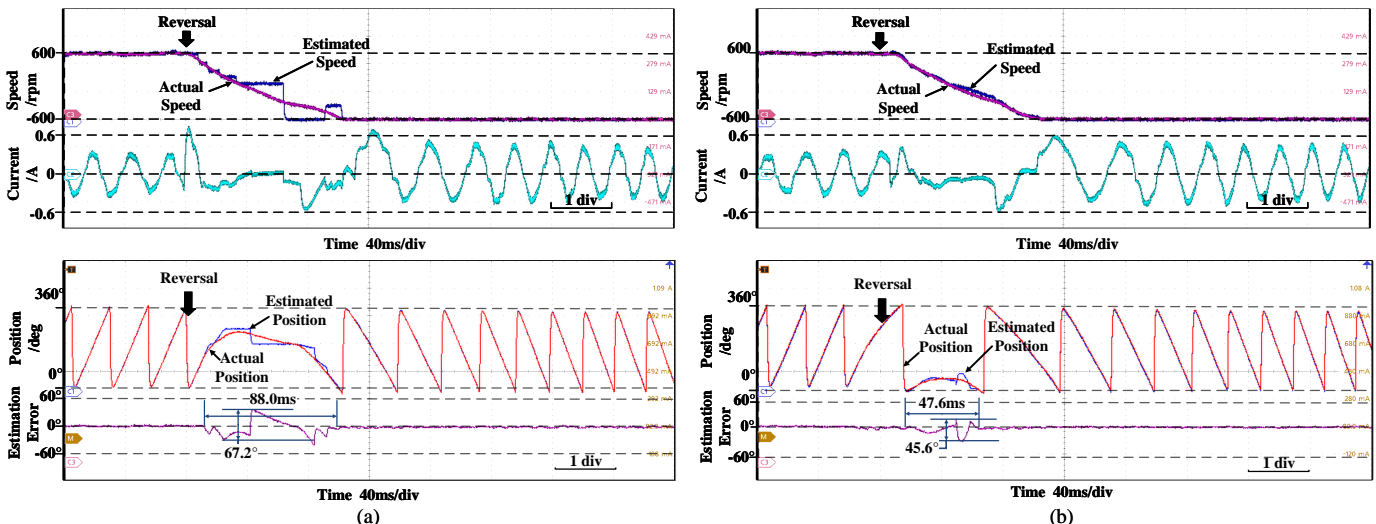


Fig. 13. Speed varied from 600 rpm to -600 rpm. (a) With the average speed method. (b) With the proposed position estimator.

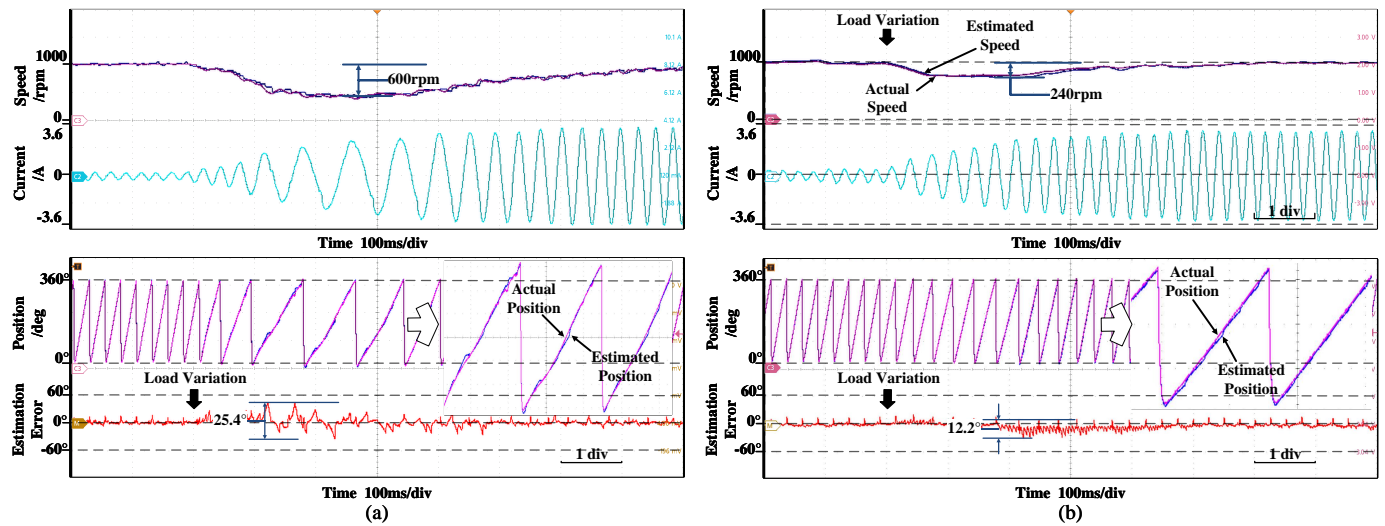


Fig. 14. Load change from 0.15 N·m to 1.15 N·m. (a) With the average speed method. (b) With the proposed position estimator.

previous sector, which will cause the estimated position to be inaccurate for a period of time. As shown in Fig. 13(a), the response of average speed method has a estimated position error up to  $67.2^\circ$ , and a convergence time up to 88.0 ms for a sudden step of speed reference from 600 rpm to -600 rpm. For comparison, as Fig. 13(b) shows, the estimated position error and the convergence time are reduced to  $67.2^\circ$  and 47.6 ms, respectively. Moreover, a smoother reversal process is achieved.

Load variation is also a common working condition in practical applications, and Fig. 14 shows the comparison of speed and estimated position using the two methods. With the average speed method in Fig. 14(a), the estimated speed responds more slowly to load variation, so the speed drop is up to 600 rpm when the load steps from 0.15 N·m to 1.0 N·m, and the estimated error of position is up to 25.4° with a convergence time longer than 800 ms. By the proposed method shown in Fig. 14(b), the speed drop caused by load is significantly reduced to 240 rpm; additionally, the response time is smaller than 500 ms and the estimation error of position is smaller than 12.2°.

## V. CONCLUSION

The installation deviation of sensors is a common problem for both BLDC and PMSM using hall sensors. In this paper, an observation function containing information of motor speed and position is constructed based on the exact discrete-time model of SPMMSM. And the rectification of estimated position error due to sensor misalignment is summarized as an optimization problem, which uses the deviation between the ideal observation value and the actual observation value to obtain the deviation angle.

Firstly, the installation misalignment of the actual hall sensors was analyzed, and it was shown that the method can well identify the installation deviation angle and calibrate it. Next, the effect of different error combinations of three hall sensors is analyzed by simulating the hall signals, and the results show that the installation asymmetry of three halls does not bring about undesirable coupling effects. Then an

improved rotor position estimator with a simple algorithm is proposed, which takes the average speed calculated by hall signals as the feedforward, and a calculated speed derived from the LUT of the observation function value is utilized to compensate for the average speed in the transient process. In the proposed estimator, a simple gain-scheduling proportional control is used to compensate for the dynamic performance while maintaining the advantages of the traditional method in the steady-state process.

The proposed method can enhance the transient performance of PMSM control using Hall-effect sensors. This method exhibits superior anti-disturbance performance and start-up capability when compared to the average speed method and other observers based on sensorless methods. Additionally, it can rectify position estimation problems caused by sensor installation misalignment.

## REFERENCES

- [1] G. Wang, M. Valla and J. Solsona, "Position sensorless permanent magnet synchronous machine drives—A review," *IEEE Trans. Ind. Electron.*, vol. 67, no. 7, pp. 5830-5842, Jul. 2020.
- [2] A. Lidozzi, L. Solero, F. Crescimbini and A. Di Napoli, "SVM PMSM drive with low resolution Hall-effect sensors," *IEEE Trans. Power Electron.*, vol. 22, no. 1, pp. 282-290, Jan. 2007.
- [3] H.-J. Ahn and D.-M. Lee, "A new bumpless rotor-flux position estimation scheme for vector-controlled washing machine," *IEEE Trans. Ind. Informat.*, vol. 12, no. 2, pp. 466-473, Apr. 2016.
- [4] N. Samoylenko, Q. Han and J. Jatskevich, "Dynamic performance of brushless DC motors with unbalanced hall sensors," *IEEE Trans. Energy Convers.*, vol. 23, no. 3, pp. 752-763, Sep. 2008.
- [5] J. Lara, J. Xu and A. Chandra, "Effects of rotor position error in the performance of field-oriented-controlled PMSM drives for electric vehicle traction applications," *IEEE Trans. Ind. Electron.*, vol. 63, no. 8, pp. 4738-4751, Aug. 2016.
- [6] A. Mousmi, A. Abbou and Y. E. Houm, "Binary diagnosis of hall effect sensors in brushless dc motor drives," *IEEE Trans. Power Electron.*, vol. 35, no. 4, pp. 3859-3868, Apr. 2020.
- [7] F. G. Capponi et al., "AC brushless drive with low-resolution Hall-effect sensors for surface-mounted PM machines," *IEEE Trans. Ind. Appl.*, vol. 42, no. 2, pp. 526-535, Mar./Apr. 2006.
- [8] M. Ebadpour, N. Amiri and J. Jatskevich, "Fast fault-tolerant control for improved dynamic performance of Hall-sensor-controlled brushless DC motor drives," *IEEE Trans. Power Electron.*, vol. 36, no. 12, pp. 14051-14061, Dec. 2021.

- [9] H.-S. Seol, J. Lim, D.-W. Kang, J.-S. Park and J. Lee, "Optimal design strategy for improved operation of IPM BLDC motors with low-resolution Hall sensors," *IEEE Trans. Ind. Electron.*, vol. 64, no. 12, pp. 9758-9766, Dec. 2017.
- [10] E. Mitronikas, D. Papathanasopoulos, G. Athanasiou and S. Tsotoulidis, "Hall-effect sensor fault identification in brushless DC motor drives using wavelets," *Proc. IEEE 11th Int. Symp. Diagnostics Elect. Mach. Power Electron. Drives*, pp. 434-440, 2017.
- [11] Z. Wu et al., "Effect of hall errors on electromagnetic vibration and noise of integer-slot inset permanent magnet synchronous motors," *IEEE Trans. Transport. Electricif.*, 2022, vol. 9, no. 1, pp. 522-533, Mar. 2022.
- [12] J. S. Park and K.-D. Lee, "Online advanced angle adjustment method for sinusoidal BLDC motors with misaligned hall sensors," *IEEE Trans. Power Electron.*, vol. 32, no. 11, pp. 8247-8253, Nov. 2017.
- [13] M. Aqil and J. Hur, "A direct redundancy approach to fault-tolerant control of BLDC motor with a damaged hall-effect sensor," *IEEE Trans. Power Electron.*, vol. 35, no. 2, pp. 1732-1741, Feb. 2020.
- [14] S. Morimoto, M. Sanada et al., "Sinusoidal current drive system of permanent magnet synchronous motor with low resolution position sensor," *Proc. IEEE IAS Annu. Meeting*, Oct 1996.
- [15] Bu Jianrong, Xu Longya, T. Sebastian and Buyun Liu, "Near-zero speed performance enhancement of PM synchronous machines assisted by low-cost Hall effect sensors," *APEC '98 Thirteenth Annual Applied Power Electronics Conference and Exposition*, vol. 1, pp. 64-68, 1998.
- [16] Z. Feng and P. P. Acarnley, "Extrapolation technique for improving the effective resolution of position encoders in permanent-magnet motor drives," *IEEE/ASME Trans. Mechatron.*, vol. 13, no. 4, pp. 410-415, Aug. 2008.
- [17] S. B. Ozturk, O. C. Kivanc, B. Atila, S. U. Rehman, B. Akin and H. A. Toliyat, "A simple least squares approach for low speed performance analysis of indirect FOC induction motor drive using low-resolution position sensor," *Proc. IEEE Int. Elect. Mach. Drives Conf.*, pp. 1-8, 2017.
- [18] Q. Ni et al., "A new position and speed estimation scheme for position control of PMSM drives using low-resolution position sensors," *IEEE Trans. Ind. Appl.*, vol. 55, no. 4, pp. 3747-3758, Jul./Aug. 2019.
- [19] L. Kreindler, I. Iacob, G. Casaru, A. Sarca, R. Olteanu and D. Matianu, "PMSM drive using digital hall position sensors for light EV applications," *Proc. 9th Int. Symp. Adv. Topics Elect. Eng.*, pp. 199-204.
- [20] C. Miguel-Espinar et al., "Accurate angle representation from misplaced Hall-effect switch sensors for low-Cost electric vehicle applications," *IEEE Trans. Ind. Appl.*, vol. 58, no. 4, pp. 5227-5237, July-Aug. 2022.
- [21] F. Giulii Capponi, G. De Donato, L. Del Ferraro, O. Honorati, M. C. Harke and R. D. Lorenz, "AC brushless drive with low-resolution hall-effect sensors for surface-mounted PM machines," *IEEE Trans. Ind. Appl.*, vol. 42, no. 2, pp. 526-535, Mar. 2006.
- [22] M. C. Harke, G. De Donato, F. G. Capponi, T. R. Tesch and R. D. Lorenz, "Implementation issues and performance evaluation of sinusoidal surface-mounted PM machine drives with Hall-effect position sensors and a vector-tracking observer," *IEEE Trans. Ind. Appl.*, vol. 44, no. 1, pp. 161-173, Jan./Feb. 2008.
- [23] X. Xu, X. Huang and Z. Li, "An improved rotor position estimation method for PMSM using low-resolution Hall-effect sensors," *ITEC Asia-Pacific 2022*, pp. 1-4, Oct 2022.
- [24] S. Kim, C. Choi, K. Lee and W. Lee, "An improved rotor position estimation with vector-tracking observer in PMSM drives with low-resolution hall-effect sensors," *IEEE Trans. Ind. Electron.*, vol. 58, no. 9, pp. 4078-4086, Sep. 2011.
- [25] L. Kovudhikulungsri and T. Koseki, "Precise speed estimation from a low-resolution encoder by dual-sampling-rate observer," *IEEE ASME Trans. Mechatron.*, vol. 11, no. 6, pp. 661-670, Dec. 2006.
- [26] A. Yoo, S.-K. Sul, D.-C. Lee and C.-S. Jun, "Novel speed and rotor position estimation strategy using a dual observer for low-resolution position sensors," *IEEE Trans. Power Electron.*, vol. 24, no. 12, pp. 2897-2906, Dec. 2009.
- [27] G. Liu, B. Chen and X. Song, "High-precision speed and position estimation based on hall vector frequency tracking for PMSM with bipolar hall-effect sensors," *IEEE Sensors J.*, vol. 19, no. 6, pp. 2347-2355, Mar. 2019.
- [28] G. De Donato, G. Scelba, M. Pulvirenti, G. Scarcella and F. G. Capponi, "Low-cost high-resolution fault-robust position and speed estimation for PMSM drives operating in safety-critical systems," *IEEE Trans. Power Electron.*, vol. 34, no. 1, pp. 550-564, Jan. 2019.
- [29] Y. Yang and Y. Ting, "Improved angular displacement estimation based on hall-effect sensors for driving a brushless permanent-magnet motor," *IEEE Trans. Ind. Electron.*, vol. 61, no. 1, pp. 504-511, Jan. 2014.
- [30] K. Liu, Z. Q. Zhu, Q. Zhang and J. Zhang, "Influence of nonideal voltage measurement on parameter estimation in permanent-magnet synchronous machines," *IEEE Trans. Ind. Electron.*, vol. 59, no. 6, pp. 2438-2447, Jun. 2012.